104 (2025) 104754

Contents lists available at ScienceDirect

Poultry Science

journal homepage: www.elsevier.com/locate/psj

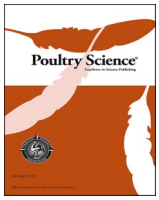

Lactobacillus salivarius metabolite succinate enhances chicken intestinal stem cell activities via the SUCNR1-mitochondria axis

Danni Luo [a,b], Minyao Zou [a,b,c], Xi Rao [d], Mingping Wei [e], Lingzhi Zhang [a,b], Yuping Hua [a,b], Lingzi Yu [a,b], Jiajia Cao [a,b], Jinyi Ye [a,b], Sichao Qi [a,b,c], Huanan Wang [a,b], Yuling Mi [a,b], Caiqiao Zhang [a,b], Jian Li [a,b,*]

[a] *MOA Key Laboratory of Animal Virology, College of Animal Sciences, Zhejiang University, Hangzhou 310058, PR China*
[b] *Department of Veterinary Medicine, College of Animal Sciences, Zhejiang University, Hangzhou 310058, PR China*
[c] *Hainan Institute of Zhejiang University, Sanya 572025, PR China*
[d] *Qingliu Animal Husbandry, Veterinary and Aquatic Products Center, Sanming 365300, PR China*
[e] *Fujian Xin Fengqiang agriculture Co., LTD, Sanming 365300, PR China*

A R T I C L E I N F O

Keywords:
Lactobacillus salivarius
Succinate
Intestinal stem cell
Mitochondria

A B S T R A C T

The activity of intestinal stem cells (**ISCs**) can be modulated by *Lactobacillus*, which subsequently affects the mucosal absorptive capacity. However, the underlying mechanisms remain unclear. In this study, a total of 189 Hy-Line Brown chickens (*Gallus*) were randomly assigned to one of seven experimental groups (n = 27 per group). These groups included a control group, a vehicle group (**MRS** group), a *Lactobacillus salivarius* group, a L. *salivarius supernatant* group, and three succinate treatment groups with various dosages. Each group was further subdivided into three replicates, with 9 chickens per replicate. The results indicate that the administration of *Lactobacillus salivarius* supernatant to laying hens notably increased the mRNA abundance of the amino acid transporters oligopeptide transporter 1 (***PepT1***) and sodium-dependent neutral amino acid transporter (***B^{0}AT***). Metabolomic analyses indicated that the supernatant contains a high concentration of organic acids. Among them, succinate could enhance mRNA abundance of *PepT1*, *B^{0}AT* and excitatory amino acid transporters 3 (***EAAT3***) both *in vivo* and *in vitro*. Accordingly, succinate could accelerate intestinal epithelial turnover, as indicated by the increased levels of cyclin-dependent kinase 2 (***Cdk2***) mRNA and proliferating cell nuclear antigen protein (**PCNA**), as well as ISC differentiation-related protein leucine-rich repeat containing G protein-coupled receptor 5 (**LGR5**). Furthermore, succinate treatment was shown to elevate the levels of mitochondrial fusion proteins optic atrophy 1 (**OPA1**) and translocase of outer mitochondrial membrane 20 (**TOMM20**), resulting in increased local ATP levels. However, pretreatment with NF-56-EJ40, a succinate receptor antagonist, attenuated the effects of succinate on OPA1, TOMM20, and ATP levels, alone with the reducing LGR5 and PCNA levels. Collectively, succinate, a metabolite of L. *salivarius*, activates the SUCNR1-mitochondria axis in ISCs, facilitating mitochondrial ATP synthesis, promoting ISC activity, and ultimately enhancing mucosal absorptive capacity.

Introduction

The intestinal mucosa is essential for nutrient absorption and defense against pathogens, relying on the continuous renewal of the intestinal epithelium. This renewal is driven by intestinal stem cells (ISCs), including active (aISC) and reserve (rISC) states, located at the base of intestinal crypts. The crypt microenvironment and gut microbiota critically regulate ISC activity and mucosal function. Studies increasingly highlight the role of lactobacilli in modulating both ISC activity and mucosal function. *Lactobacillus reuteri* promotes the proliferation of intestinal epithelial cells by upregulating the expression of R-spondins, thereby activating the Wnt/β-catenin signaling pathway (Wu et al., 2020). *Lactobacillus rhamnosus* GG promotes the repair of damaged mouse intestinal mucosa by enhancing the regenerative capacity of ISCs

Scientific section: Molecular and Cellular Biology

* Corresponding author.
E-mail address: lijiannp@zju.edu.cn (J. Li).

https://doi.org/10.1016/j.psj.2024.104754
Received 7 October 2024; Accepted 30 December 2024
Available online 31 December 2024

(Chen et al., 2023). In our previous study, it was demonstrated that *Lactobacillus salivarius* enhances the activity of ISCs to promote epithelial turnover and enhance the intestinal mucosal absorptive capacity (Liu et al., 2022). However, the underlying mechanisms by which L. *salivarius* regulates ISCs remain undefined.

Organic acids produced by *Lactobacillus* metabolism can regulate intestinal mucosal function by inhibiting pathogen adhesion, reducing enterotoxin synthesis, and alleviating intestinal inflammation (Khan et al., 2022). Among the organic acids, succinate plays a crucial role in regulating mucosal function. It promotes the expansion of Tuft cells to suppress mouse ileitis (Banerjee et al., 2020), enhances the proliferation and differentiation of ISCs in laying hens (Zhou et al., 2022), and improves the intestinal mucosal barrier function in pigs by upregulating the expression of tight junction proteins, such as zona occludens 1 (Li et al., 2019). In contrast, some studies suggest that succinate exacerbates intestinal damage in mice with necrotizing enterocolitis by activating the hypoxia-inducible factor 1α (**HIF-1α**) signaling pathway (Yan et al., 2022). However, the regulatory mechanism of ISCs' activity by succinate remains unclear.

Numerous studies have indicated that succinate regulates cellular functions through two distinct pathways. One is the transport carrier-mediated pathway (Connors et al., 2018), the other one is SUCNR1 (**G protein-coupled receptor 91**)-mediated pathway (Villanueva-Carmona et al., 2023). Through SUCNR1-mediated pathway, succinate regulates leptin production in adipocytes, potentially impacting metabolic health based on nutritional status (Villanueva-Carmona et al., 2023). Succinate and SUCNR1 are upregulated in Crohn's disease fistulas, where they activate Wnt signaling and induce epithelial-to-mesenchymal transition. This highlights their potential as targets for fistula prevention (Ortiz-Masiá et al., 2020). However, the pathway through which succinate influences ISCs' activity remains elusive.

Mitochondrial dynamics are key to ISC regulation. In *Drosophila*, ISC differentiation involves mitochondrial fusion, and inhibiting fusion reduces ISC differentiation activity (Deng et al., 2018). *Escherichia* coli-LF82 adheres to intestinal epithelial cells, activating fission-related protein 1 (**DRP1**) to induce mitochondrial fission, releasing cytochrome C, and impairing intestinal epithelial integrity (Mancini et al., 2021). Bile acids target mitofusin 2 (**MFN2**) promote mitochondrial fusion in macrophages, enhancing oxidative phosphorylation (**OXPHOS**) levels, and boosting their immune response (Che et al., 2023). Aspartate promotes mitochondrial fusion, boosts energy metabolism, and supports ISCs proliferation and differentiation, helping repair colonic epithelial damage (Wang et al., 2022). In skeletal and cardiac muscle, optic atrophy 1 (**OPA1**) mediates inner mitochondrial membrane fusion, improving OXPHOS efficiency (Noone et al., 2022). In contrast, deletion of OPA1 and mitochondrial assembly regulatory factor (**MARF**) causes mitochondrial fragmentation, significantly reducing *Drosophila* neural stem cell differentiation capacity (Dubal et al., 2022). However, the signaling pathway through which succinate influences mitochondrial dynamics and subsequently regulates ISC activity remains to be elucidated.

Taken together, this study will confirm the regulation of succinate, a metabolite of L. *salivarius*, on mucosal absorptive capacity, intestinal epithelial turnover, and ISCs' activity. Furthermore, this study focuses on mitochondrial dynamics, exploring the mechanisms by which succinate modulates ISC activity.

Materials and methods

Animals

A total of 189 Hy-Line Brown chickens (*Gallus*), 450 days old, were randomly divided into seven groups. These groups included a control group, a vehicle group (**MRS** group), L. *salivarius* group, L. *salivarius* supernatant group, and three succinate groups, with 27 chickens per group. Each experimental group of 27 chickens was randomly divided into three replicates, with each replicate consisting of 9 chickens. The control group was fed a basal diet. Chickens in the L. *salivarius* group, L. *salivarius* supernatant group, and MRS group were fed a basal diet containing L. *salivarius* (CGMCC 1.1881, 10^8 CFU/chick/day) or supernatant of L. *salivarius* or MRS at an equal volume for 14 consecutive days. The supernatant of L. *salivarius* was obtained by centrifugting of the L. *salivarius* suspension at 1250 × g for 2 min, followed by bacteriological filtration using a 0.22 μm syringe filter. The succinate groups received a diet supplemented with succinate (MB4700-1, MeilunBio, Dalian, China) at concentrations of 5 mg/Kg BW, 10 mg/Kg BW, or 20 mg/Kg BW, respectively. At the end of the feeding trial, intestinal tissue and crypts were collected from nine individuals. This study was conducted following the *Guiding Principles for the Care and Use of Laboratory Animals* as adopted by Zhejiang University. Approval for the experimental procedures was granted by *Zhejiang University's Committee on the Ethics of Animal Experiments* (Approval No. 14933).

Intestinal crypts isolation and enteroids culture

To study the changes in ISC activity *in vitro*, the intestinal crypts were isolated using a previously published method (Li et al., 2018). Briefly, the small intestine was initially cut into 2-3 cm lengths after making a longitudinal incision. Afterward, the villus was carefully removed, followed by rinsing with PBS. Subsequently, the segments were shaken in a 2 mM EDTA (pH 7.4). The mixture was then filtered through a 70 μm nylon mesh cell strainer (352360, Corning, NY, USA), followed by centrifugation of the suspension to obtain the crypts. These purified crypts were used to evaluate mRNA levels, protein levels, and for enteroid culturing.

For the enteroids culture, sterile isolated intestinal crypts were mixed with Matrigel (3533-010-02, R&D Systems, MN, USA) and then dropped on a flat-bottom plate to form hemispherical droplets. After the Matrigel solidified, a complete medium containing R-Spondin 1, Noggin, and EGF was added. The enteroids were cultured in an environment maintained at 38°C with 5 % CO_2. Succinate was added and cultured for 48 h. To analyze the pathway by which succinate regulates ISC activity, the antagonist of SUCNR1, NF-56-EJ40 (HY-130246, MedChemExpress, Shanghai, China), was added to the enteroids 30 min prior to succinate treatment. At the end of the trial, enteroids were extracted from the Matrigel using Cell Recovery Solution (354253, Corning, NY, USA) for transcriptomic analysis, mRNA transcription, and protein expression assays.

Western blot (WB)

Total protein was extracted from intestinal tissue or crypts using RIPA buffer (P0013B, Beyotime, Shanghai, China). The protein concentration was determined using the BCA protein assay kit (A045-3, Nanjing Jiancheng Bioengineering Institute, Nanjing, China). The extracted proteins were diluted with Protein Loading Buffer (FD006, Fdbio, Hangzhou, China) and boiled at 95°C for 15 min. A 30 μg of total proteins were separated by SDS-PAGE and then transferred to a 0.22 μm PVDF membrane (Millipore, MA, USA). The membrane was blocked with 5 % skimmed milk at RT for 1.5 h, followed by overnight incubation at 4°C with primary antibodies: anti-SDHA (ET1703-40, HuaBio, Hangzhou, China), anti-WNT1 (ER65317, HuaBio, Hangzhou, China), anti-COX5B (HA500163, HuaBio, Hangzhou, China), anti-TOMM20 (ET1609-25, HuaBio, Hangzhou, China), anti-PCNA (ab29, Abcam, Cambridge, UK), anti-LGR5 (customization, HuaBio, Hangzhou, China), anti-OPA1 (BSN8818, Baseniao, Hangzhou, China), or anti-β-actin (AC026, Abclonal, Wuhan, China). After rinsing in PBS, the membrane was incubated at RT for 1 h with HRP-conjugated anti-rabbit IgG (HA1001, HuaBio, Hangzhou, China) or anti-mouse IgG (HA1006, HuaBio, Hangzhou, China). The blots were detected using the SuperPico ECL chemiluminescence kit (E422-01, Vazyme, Nanjing, China) and

Table 1
Primers for PCR analysis.

Genes	Accession No.	Primer sequences (5′ - 3′)	Product (bp)
Suclg2	NM_001006141.2	F: TGGCGGTATCGTGAACTGTG R: TGACCACCAGAGGCACTTTC	86
Sirt5	XM_046911394.1	F: CTATGCGACCTCTGCTTGGT R: CCTGAACCTGTCTGTAGCGG	138
Cox8a	XM_040694276.2	F: CAATAAAGGCCGCTTACGCC R: ACATGATGACGTCAACCCCC	89
Sdha	NM_001277398.1	F: ACCATTTACCACCCCAGCAG R: ACCGTAGGCAAAACGGGAAT	112
β-cantenin	XM_046910392.1	F: GCAACAGCAGTTTGTGGAGG R: CGTGCAAGAATATGCAGGGC	78
Tnf-α	NM_204267.1	F: ACCCGTAGTGCTGTTCTATGACC R: TGTTCCACATCTTTCAGAGCATC	192
Il-β	NM_204524.2	F: CTGGGCATCAAGGGCTACAA R: CGGTAGAAGATGAAGCGGGT	131
Il-6	NM_204628.2	F: CTCCTCGCCAATCTGAAGTC R: GGCACTGAAACTCCTGGTCT	138
Lgr5	XM_425441.7	F: CATACATTCCTAAGGGAGCAT R: GTGTCTAAGGGAGACCAAACC	191
Bax	XM_01S290060.2	F: GGATGACAGGAAAGTACGGCA R: TCACCAGGAAGACAGCGTAT	173
Cdk2	NM_001199857.1	F: TCCGTATCTTCCGCACGTTG R: GCTTGTTGGGATCGTAGTGC	183
PepT1	NM_204365	F: GATCACTGTTGG*CAT*GTTCCT R: *CAT*TCG*CAT*TGCTATCACCTA	146
B^0AT	XM_419056	F: AATGGGACAACAAGGCTCAG R: CAAGATGAAGCAGGGGGATA	165
EAAT3	XM_424930	F: AAAATGGGAGACAAAGGACAA R: ACGAAAGATTTCCCAGTCCTC	159
Wnt3a	NM_001171601.1	F: CTTCTTCAAGGCTCCGACTG R: GGCACTTCTCTTTCCGTTTC	200
GAPDH	NM_204305	F: GATGGGTGTCAACCATGAGAAA R: CAATGCCAAAGTTGTCATGGA	116

visualized with the Bio-Rad ChemiDocTM Touch Imaging System (CA, USA). The densitometry of the blots was analyzed using ImageJ and normalized to β-actin.

Quantitative real-time PCR (qPCR)

Total RNA was extracted from intestinal tissue or crypts using FreeZol Reagent (R711-01, Vazyme, Nanjing, China) and reverse transcribed into cDNA using the HiScript III All-in-one RT SuperMix kit (R333-01, Vazyme, Nanjing, China). Using cDNA as a template, reactions were performed on the Bio-Rad CFX96 Touch Real-Time PCR machine (CA, USA). The reaction system included 1.5 μL of cDNA, 400 nM primers (Table 1), and 7.5 μL of 2 × SYBR qPCR Master Mix (Q711-02, Vazyme, Nanjing, China). The reaction conditions were as follows: 95°C for 30 s; 95°C for 10 s; 60°C for 30 s, for 40 cycles. *Gadph* was used for normalization. Data analysis was performed using the comparative cycle threshold method ($2^{-\triangle\triangle Ct}$). The experiment was biologically replicated in triplicate, with all samples being technically replicated in triplicate.

Intestinal flora assay and untargeted metabolomic analysis

For 16S rDNA V3-V4 region assay, intestinal contents from six individuals in each group were aseptically collected, frozen in dry ice, and sent to a commercial company (Novogene Co. Ltd, Beijing, China). Briefly, genomic DNA was extracted from the intestinal contents, followed by amplification of the V3-V4 region of the 16S rDNA. Amplicons were pooled equimolarly and sequenced in paired-end (2 × 250) on an Illumina MiSeq platform. Raw FASTQ files were demultiplexed and quality-filtered using QIIME. Operational Taxonomic Units (OTUs) were identified at a 97 % similarity cutoff using UPARSE (version 7.1), with the removal of chimeric sequences by UCHIME. Taxonomic classification was conducted using the RD *P*-value < Classifier against the Silva (SSU115) 16S rRNA genes database with a confidence threshold of 70 %.

To identify the metabolites of L. *salivarius*, the L. *salivarius* supernatant was sent to a commercial company (Novogene Co. Ltd., Beijing, China) for untargeted metabolomic analysis. Samples were freeze-dried, mixed with 80 % methanol, and then centrifuged. LC-MS/MS analysis was conducted using an ultra-high performance liquid chromatography (UHPLC) system and an Orbitrap mass spectrometer. Data were processed using Compound Discoverer 3.1 for peak analysis and normalization. Metabolites were identified using the KEGG database. Those with a VIP-value > 1 and < 0.05, and an FC-value ≥ 2 or ≤ 0.5, were considered statistically different.

RNA sequencing

To identify differentially expressed genes in the enteroids, samples from three biological replicates per group were collected, frozen on dry ice, and sent to a commercial company (Novogene Co. Ltd, Beijing, China) for analysis. The process involved extracting total RNA, followed by transcriptome sequencing on the Illumina platform. The identification of genes that were significantly differentially expressed was performed using the EdgeR algorithm, a feature integrated into the CLC Genomics Workbench (Qiagen, Hilden, Germany).

To ensure the quality and reliability of data analysis, reads containing adapters, uncertain nucleotide information (denoted as N), and low-quality were eliminated. The reference genome index was constructed using HISAT2 v2.0.5, and clean paired-end reads were aligned to the chicken reference genome using HISAT2 v2.0.5. Differential expression analysis between two comparison groups was conducted using DESeq2 software (version 1.20.0), and the resulting *P*-values were adjusted using Benjamini and Hochberg's method to control the false discovery rate. Genes with an adjusted *P*-value < 0.05, as identified by DESeq2, were designated as differentially expressed. GO enrichment analysis and KEGG enrichment analysis of differentially expressed genes were conducted using the clusterProfiler R package.

Immunofluorescence

For the localization analysis of proteins in enteroids, immunofluorescence was performed. Briefly, the enteroids were fixed with 4 % PFA for 20 min, followed by blocking with 10 % goat serum (AR0009, Boster, Wuhan, China) for 20 min. Then, samples were incubated overnight at 4°C with the following primary antibodies: anti-TOMM20 (ET1609-25, HuaBio, Hangzhou, China) or anti-LGR5 (customized, HuaBio, Hangzhou, China). After rinsing with PBS, the samples were incubated with 594-conjugated goat anti-rabbit IgG (AS039, Abclonal, Wuhan, China) or 488-conjugated goat anti-rabbit IgG (AS053, Abclonal, Wuhan, China) at 37°C for 1 h. Subsequently, the enteroids were incubated with DAPI at 37°C for 20 min. Imaging was captured using a Nikon A1R confocal laser scanning microscope (Tokyo, Japan) or an Olympus IX81-FV1000 confocal laser scanning microscope (Tokyo, Japan).

ATP chemiluminescence assay

The ATP levels were measured using the ATP chemiluminescence assay kit (E-BC-F002, Elabscience, Wuhan, China). In brief, the enteroid samples collected from each group were weighed for wet weight and placed in 2 mL EP tubes. Each tube was added 0.45 mL of reagent I and then incubated in a boiling water bath for 10 min. After cooling under running water, the tubes were centrifuged at 4°C, 10,000 × g, for 10 min, and the supernatant was collected to determine ATP content. The reaction of ATP with luciferin, catalyzed by luciferase, emits light that can be detected to calculate the ATP content.

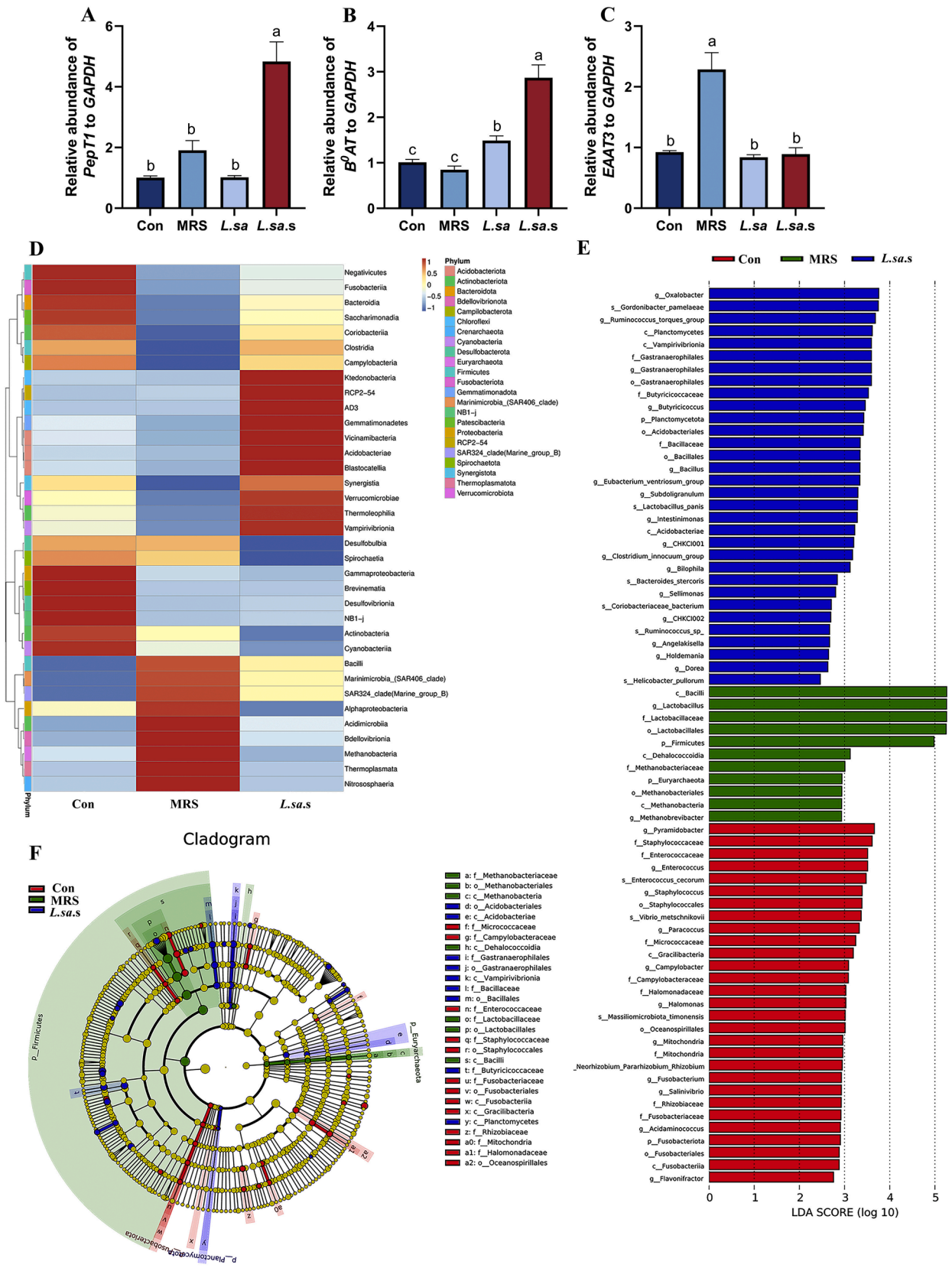

Figure 1. The supernatant of L. *salivarius* improved intestinal mucosal absorptive capacity and host's intestinal flora. Laying hens were fed the supernatant of L. *salivarius* for 14 consecutive days. (A-C) Histograms represent the alterations in mRNA abundance of amino acid transporters *PepT1, B^0AT*, and *EAAT3* in the jejunum. The data is presented as mean ± standard deviation ($n = 6$). Columns without common letters indicate significant differences (P-value < 0.05) among the various treatments. (D) Cluster heatmaps of species abundance for the top 35 at the phylum level. (E-F) Histograms and cladograms represent the values of linear discriminant analysis (LDA). Con, chickens were fed a basal diet; MRS, as vehicle group, chickens were fed a basal diet containing MRS; L. *sa.*, chickens were fed a basal diet containing L. *salivarius*; L. *sa.* s, chickens were fed a basal diet containing L. *salivarius* supernatant.

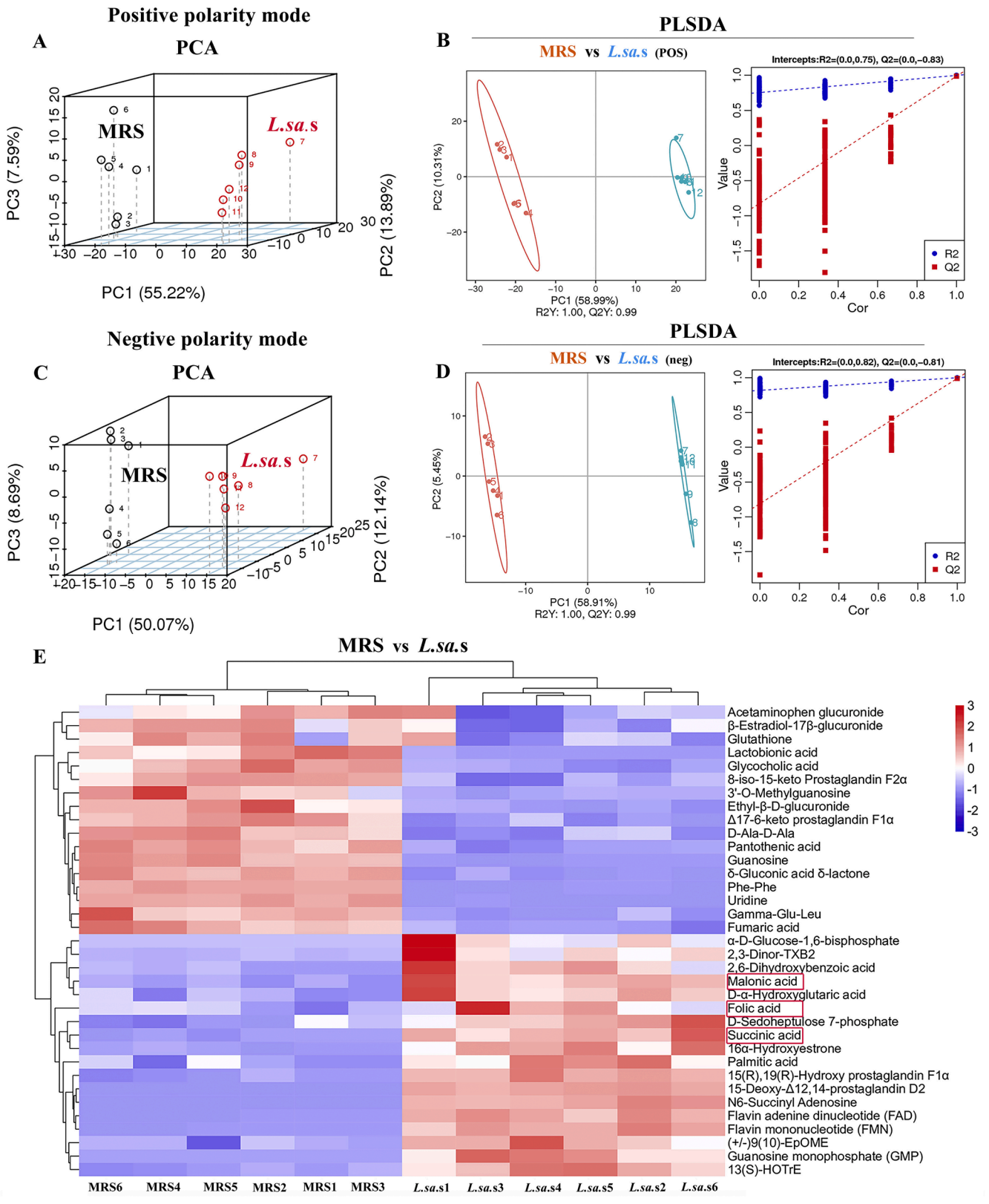

Figure 2. Screening for the essential metabolite in the L. *salivarius* supernatant regulates intestinal mucosal absorptive capacity. Untargeted metabolomics analysis was conducted on the L. *salivarius* supernatant, with MRS used as the vehicle group. (A, C) The PCA results in both negative and positive polarity modes. (B, D) The PLSDA results in both negative and positive polarity modes. (E) Hierarchical clustering analysis of differential metabolites between the MRS and the L. *salivarius* supernatant.

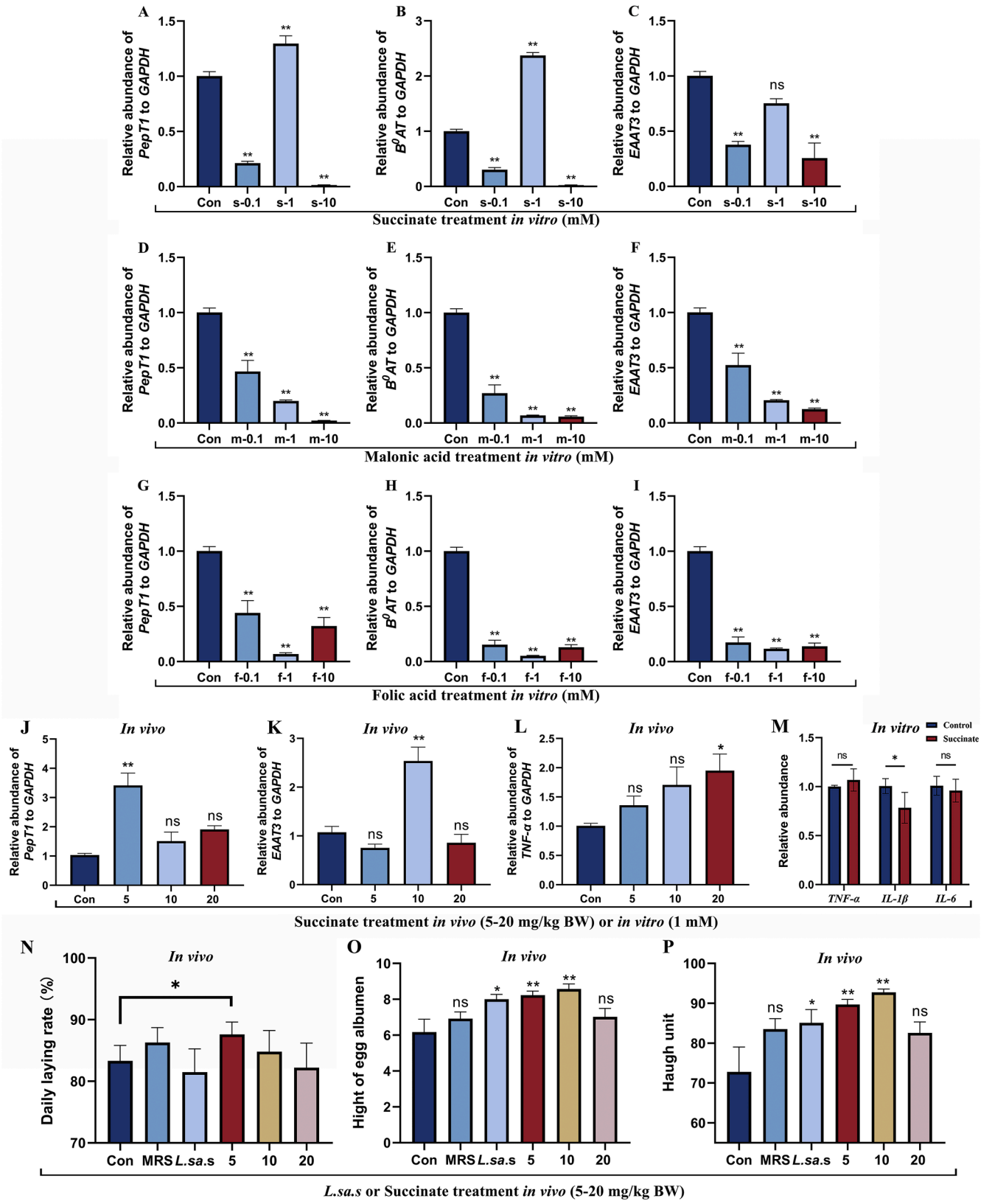

Figure 3. Screening effective organic acids and determining their optimal dosage to enhance intestinal mucosal absorptive capacity. Histograms represent the alterations in mRNA abundance of amino acid transporters in the enteroids treated with Succinate (A-C), Malonic acid (D-F), or Folic acid (G-I) at dosages ranging from 0.1 mM to 10 mM, respectively, for 48 h. (J-L) Histograms represent the alterations in mRNA abundance of *PepT1, EAAT3* and *Tnf-α* in the jejunum of laying hens fed succinate at dosages ranging from 5 to 20 mg/kg BW. (M) Histograms represent the alterations in mRNA abundance of *Tnf-α, Il-1β*, and *Il-6* in enteroids treated with 1 mM succinate. (N) The daily egg production rate of each experimental group in *vivo*. (O) The height of eggs albumen from each experimental group *in vivo*. (P) The Haugh unit of eggs from each experimental group *in vivo*. The data is presented as mean ± SEM. ns, no significant difference compared to the control group, * *P*-value < 0.05 compared to the control group, ** *P*-value < 0.01 compared to the control group.

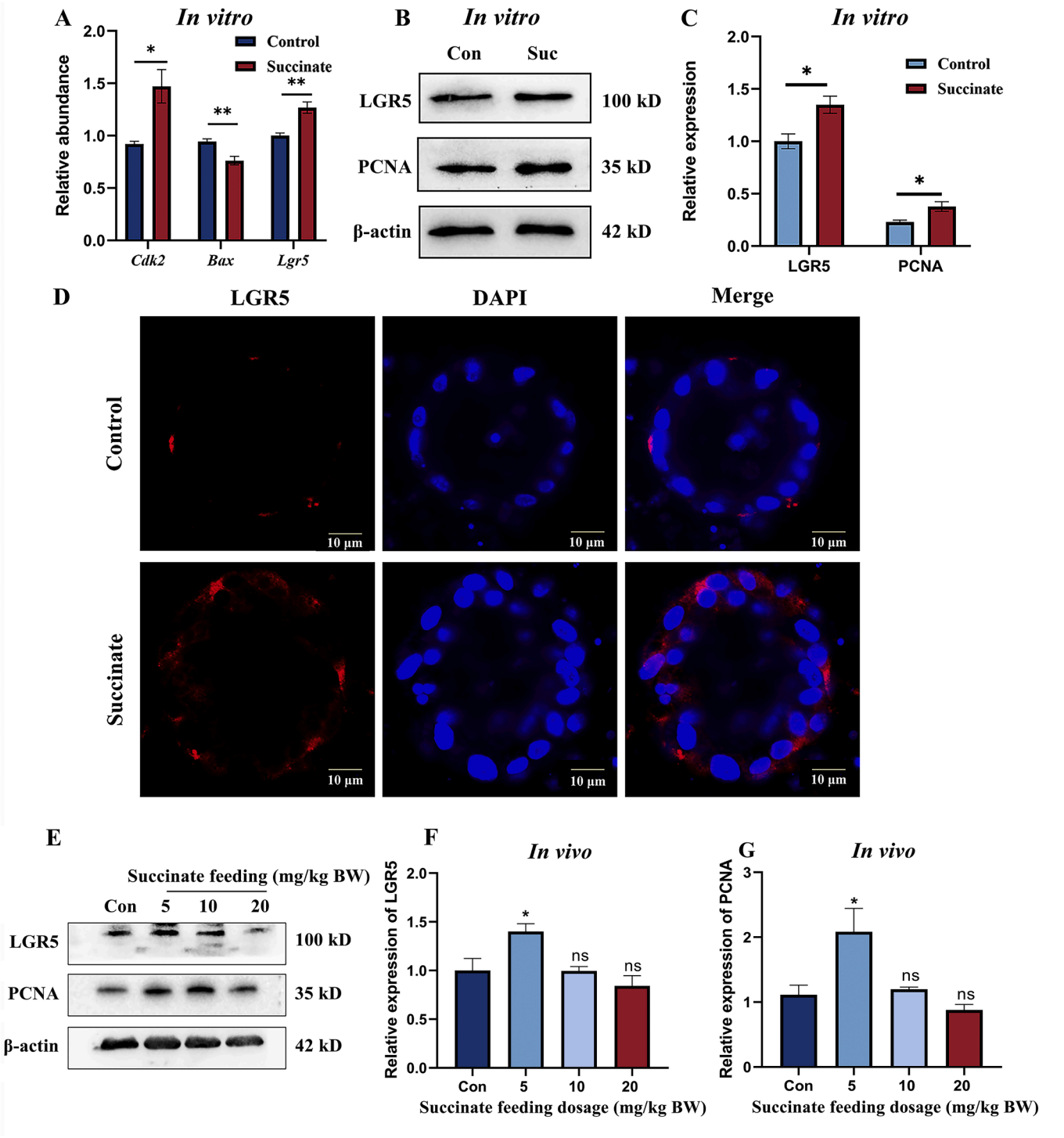

Figure 4. Succinate promotes intestinal epithelial turnover and ISC activities. (A) Histogram represents the alterations in mRNA abundance of *Cdk2, Bax,* and *Lgr5* in enteroids treated with 1 mM succinate. (B, C) Western blot analysis of LGR5 and PCNA proteins in enteroids treated with 1 mM succinate. (D) The immunofluorescent staining of LGR5 protein in enteroids, scale bar = 10 μm. (E-G) Western blot assay of LGR5 and PCNA proteins in the intestinal crypts of laying hens fed with succinate at varying dosages. The data is presented as mean ± standard deviation ($n = 3$). ns, no significant difference compared to the control group, * P-value < 0.05 compared to the control group, ** P-value < 0.01 compared to the control group.

Statistical analysis

Statistical analysis was conducted using GraphPad Prism version 9.4.0. Outliers were identified and removed from the experimental raw data following the interquartile range principle. The Shapiro-Wilk test was used to assess the normality of the data. For comparing two groups, the student's T-test was applied to data with a normal distribution, while the Mann-Whitney U test was used for data with an abnormal distribution. In analyses involving multiple groups with normally distributed data, variance homogeneity was evaluated using the Levene test. Based on this evaluation, a one-way ANOVA and LSD post hoc tests (assuming equal variances) or the Welch test and Dunnett's T3 post hoc tests (not assuming equal variances) were applied. For comparisons among multiple groups with abnormally distributed data, the Kruskal-Wallis H test

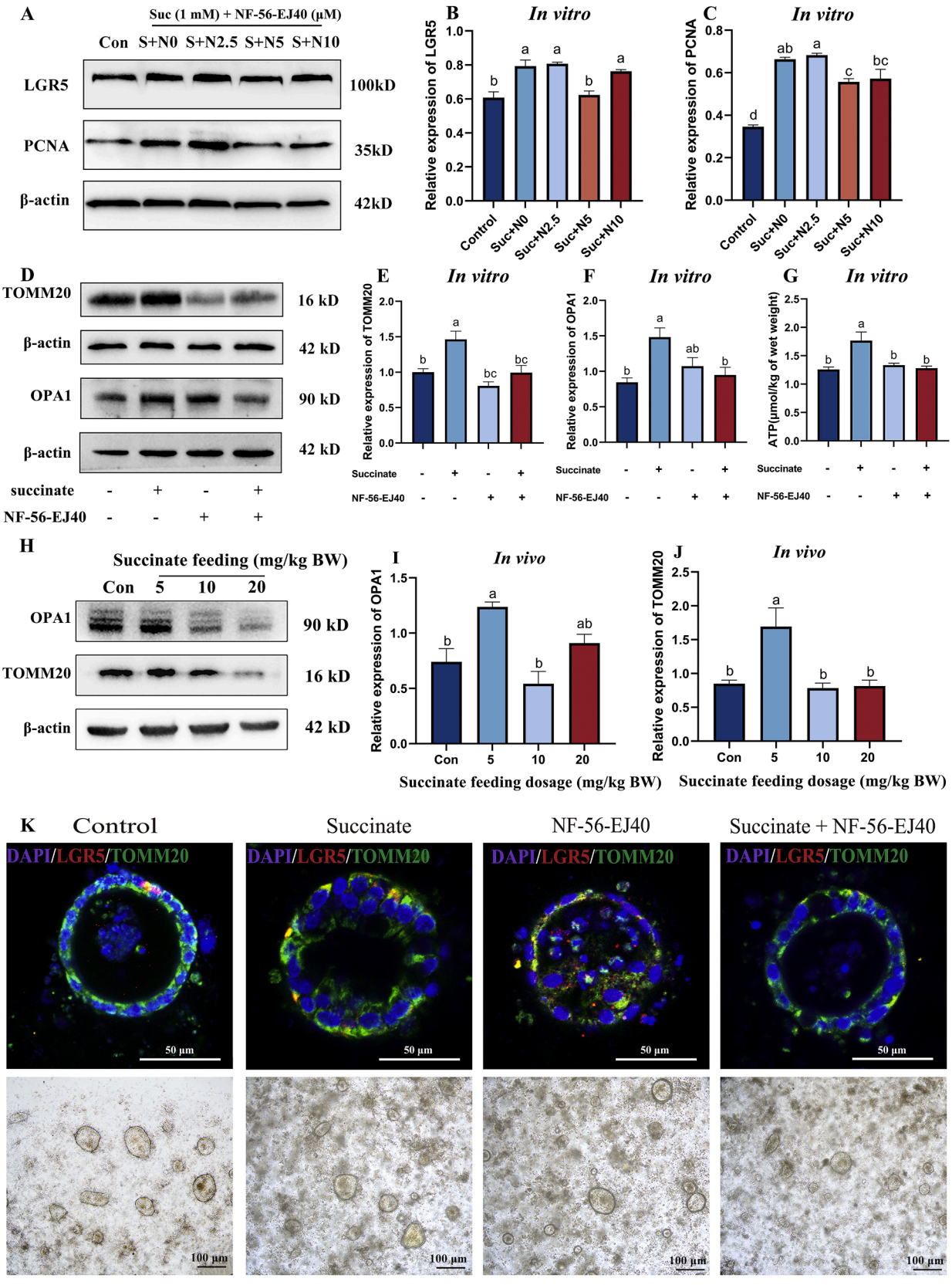

Figure 5. SUCNR1 mediates the regulation of succinate on ISC activity. The enteroids were pre-treated with the SUCNR1 antagonist NF-56-EJ40 for 30 min, followed by 1 mM succinate treatment for 48 h. (A-C) Western blot assay of LGR5 and PCNA proteins in enteroids. (D-G) Western blot analysis of OPA1 and TOMM20 proteins in enteroids. (H-J) Western blot assay of OPA1 and TOMM20 proteins in the intestinal crypts of hens that were fed with succinate at varying dosages. (K) The immunofluorescent co-staining of LGR5 and TOMM20 in enteroids, scale bar = 50 μm or 100 μm. The data is presented as mean ± standard deviation ($n = 3$). Columns without common letters indicate significant differences (P-value < 0.05) among various groups.

was utilized. A P-value < 0.05 was considered statistically significant.

Results

The supernatant of L. salivarius improved mucosal absorptive capacity and intestinal flora

To analyze the impact of the fermentation supernatant of L. *salivarius* on the intestinal mucosal absorptive capacity, laying hens were fed the fermentation supernatant of L. *salivarius* for 14 days. The analysis of amino acid transporters in the jejunum (Fig. 1A to C) indicated that the fermentation supernatant of L. *salivarius* dramatically increased the mRNA abundance of *PepT1* (by 374.47 %, P-value = 0.0247) and B^0AT (by 237.50 %, P-value = 0.0024) compared to the MRS group. Furthermore, the composition of the host's intestinal microbiota was determined using a 16S rDNA assay. Non-metric multidimensional scaling (**NMDS**) analysis and the Shannon index showed that versus the MRS group, the community composition structure and diversity in the L. *salivarius* supernatant group were distinct and remarkably higher. Species abundance cluster heatmaps of the top 35 ranked microbial groups at the phylum level (Fig. 1D) revealed that, when compared with the MRS group, the L. *salivarius* supernatant could reduce intestinal pathogenic bacteria (such as *Desulfovibrio*), while increasing beneficial bacteria (such as *Verrucomicrobia*). At the genus level, histograms and cladograms of the linear discriminant analysis (**LDA**) values (Fig. 1E and F) revealed noticeable variations among various groups. Particularly, *Oxalobacter, Ruminococcus, Gastranaerophilales*, and *Butyricicoccus* exhibited statistical significance in the L. *salivarius* supernatant group. These results suggest that the supernatant of L. *salivarius* could improve the host's intestinal mucosal absorptive capacity and improve the intestinal flora.

Succinate in the supernatant of L. salivarius regulates mucosal absorptive capacity

To identify the critical metabolite in the L. *salivarius* supernatant that regulates mucosal absorptive capacity, we conducted an untargeted metabolomic analysis on the fermentation supernatant of L. *salivarius*. The results of the principal component analysis (**PCA**, Fig. 2A and C) demonstrated observable differences in metabolites between L. *salivarius* and MRS in both negative and positive polarity modes. The partial least squares discriminant analysis (**PLSDA**, Fig. 2B and D) confirmed that there was no overfitting in either polarity mode, indicating that our data are robust and suitable for sample characterization. Hierarchical clustering analysis of differential metabolites revealed that, versus the MRS, L. *salivarius* supernatant exhibited a high abundance of organic acids, including malonic acid, folic acid, and succinic acid (Fig. 2E, red frame).

To further identify the key metabolites that could enhance ISC activity, the enteroids were treated with succinate, malonic acid, or folic acid at concentrations ranging from 0.1 mM to 10 mM. It was demonstrated that 1 mM succinic acid can increase the mRNA abundance of oligopeptide transporter 1 (***PepT1***) by 29.35 % (P-value = 0.0391) and sodium-dependent neutral amino acid transporter (***B^0AT***) by 137.07 % (P-value < 0.0001) in enteroids (Fig. 3A-C). In contrast, malonic acid and folic acid exhibited inhibitory effect on amino acid transport (Fig. 3D-I). Parallelly, *in vivo*, succinate feeding increased the *PepT1* mRNA abundance (by 229.8 %, P-value = 0.0002) at 5 mg/kg BW and the excitatory amino acid transporters3 (***EAAT3***) mRNA abundance (by 136.26 %, P-value < 0.0001) at 10 mg/kg BW (Fig. 3J and K). Moreover, it was demonstrated that succinate at the optimal dosage presented no adverse effects on chickens, as there was no prominent increase in pro-inflammatory factors *Tnf-α, Il-1β,* and *Il-6* detected both *in vivo* and *in vitro* (Fig. 3L and M). Simultaneously, we conducted an *in vivo* feeding experiment, and the results showed that the egg quality of the L. *salivarius* supernatant group, 5 mg/kg BW group, and 10 mg/kg BW group was significantly improved (Fig. 3O-P). Only the 5 mg/kg BW group showed a significant increase in egg production rate, with a 5.14 % improvement compared to the control group (*P-value* = 0.0273). In contrast, the other treatment groups did not show any significant difference in egg production rate compared to the control group. Additionally, the Haugh unit of the 5 mg/kg BW group increased significantly by 23.26 % (*P-value* = 0.0034), and the 10 mg/kg BW group also showed a significant increase of 27.43 % (*P-value* = 0.0005). Regarding albumen height, the 5 mg/kg BW group showed a significant increase of 33.51 % (*P-value* = 0.0052), while the 10 mg/kg BW group demonstrated a significant increase of 38.92 % (*P-value* = 0.0010). These results suggested that succinate may be the key effector component by which L. *salivarius* enhances mucosal absorptive capacity.

Succinate enhances the turnover of intestinal epithelium and the activity of ISC

In light of the pivotal role of intestinal epithelial turnover in mucosal function, succinate was administered both *in vivo* and *in vitro* to identify its effects on epithelial turnover. The analysis of the epithelial turnover rate revealed that, following succinate treatment, there was a considerable increase in the mRNA abundance of cyclin dependent kinase 2 (***Cdk2***) and ISC differentiation-related gene leucine-rich repeat containing G protein-coupled receptor 5 (***Lgr5***) in the enteroids, while the mRNA abundance of the apoptosis-related gene *Bcl-2* associated X (***Bax***) significantly decreased (Fig. 4A). As ISCs are foundamental to mucosal turnover, localization analysis of ISC in the enteroids revealed that $LGR5^+$ ISCs are dispersed throughout the epithelium of enteroids (Fig. 4D). Higher protein levels of LGR5 (increased by 34.93 % vs. the control group, P-value = 0.0315) and Proliferating cell nuclear antigen protein (**PCNA**) (increased by 44.26 % vs. the control group, P-value = 0.0300) were detected in the enteroids after succinate treatment (Fig. 4B and C). Simultaneously, *in vivo*, the protein levels of LGR5 and PCNA in the intestinal crypt profound increased by 40.07 % (P-value = 0.0405) and 87.30 % (P-value = 0.0224) upon succinate feeding at 5 mg/kg BW (Fig. 4E-G). These results suggest that succinate, a crucial metabolite found in the supernatant of L. *salivarius*, can enhance ISC activity, thereby promoting intestinal epithelial turnover.

SUCNR1 mediates the regulation of succinate on ISC activity

To analyze the pathway through which succinate regulates the activity of ISCs, an SUCNR1 antagonist (NF-56-EJ40) was administered to enteroids. To identify the optimal dosage at which NF-56-EJ40 blocks the effect of succinate, the enteroids were pre-treated with NF-56-EJ40 at dosages of 2.5 μM, 5 μM, or 10 μM for 30 min. Subsequently, 1 mM of succinate was added for 48 h. As shown in Fig. 5A-C, upon pre-treating NF-56-EJ40 with 5 μM, the promotion of succinate on LGR5 and PCNA protein levels significantly decreased by 21.30 % (P-value = 0.0052) and 16.12 % (P-value = 0.0391), respectively. Therefore, 5 μM was selected as the optimal dosage for NF-56-EJ40 to inhibit the regulatory effect of succinate on ISC activity.

Since mitochondria play a crucial role in determining the fate and function of cells, we analyzed the impact of succinate on mitochondrial dynamics and function. In enteroids, compared to the control group, succinate considerably upregulated the protein levels of Translocase of outer mitochondrial membrane 20 (**TOMM20**) by 46.34 % (P-value = 0.0213) and OPA1 by 75.28 % (P-value = 0.0141), and raised the ATP content by 40.38 % (P-value = 0.0110) (Fig. 5D-G). These findings were consistent with the *in vivo* results, showing that succinate feeding at a dosage of 5 mg/kg BW considerably increased the protein levels of OPA1 and TOMM20 by 66.92 % (P-value = 0.0433) and 99.44 % (P-value = 0.0111) in the intestinal crypts (Fig. 5H-J). However, upon pre-treating the antagonist in enteroids, the effect of succinate on OPA1 protein level, TOMM20 protein level, and ATP content decreased by 35.91 % (P-value = 0.0354), 31.77 % (P-value = 0.0016) and 27.53 % (P-value = 0.0140) compared to succinate treatment alone (Fig. 5D-G). Furthermore, co-

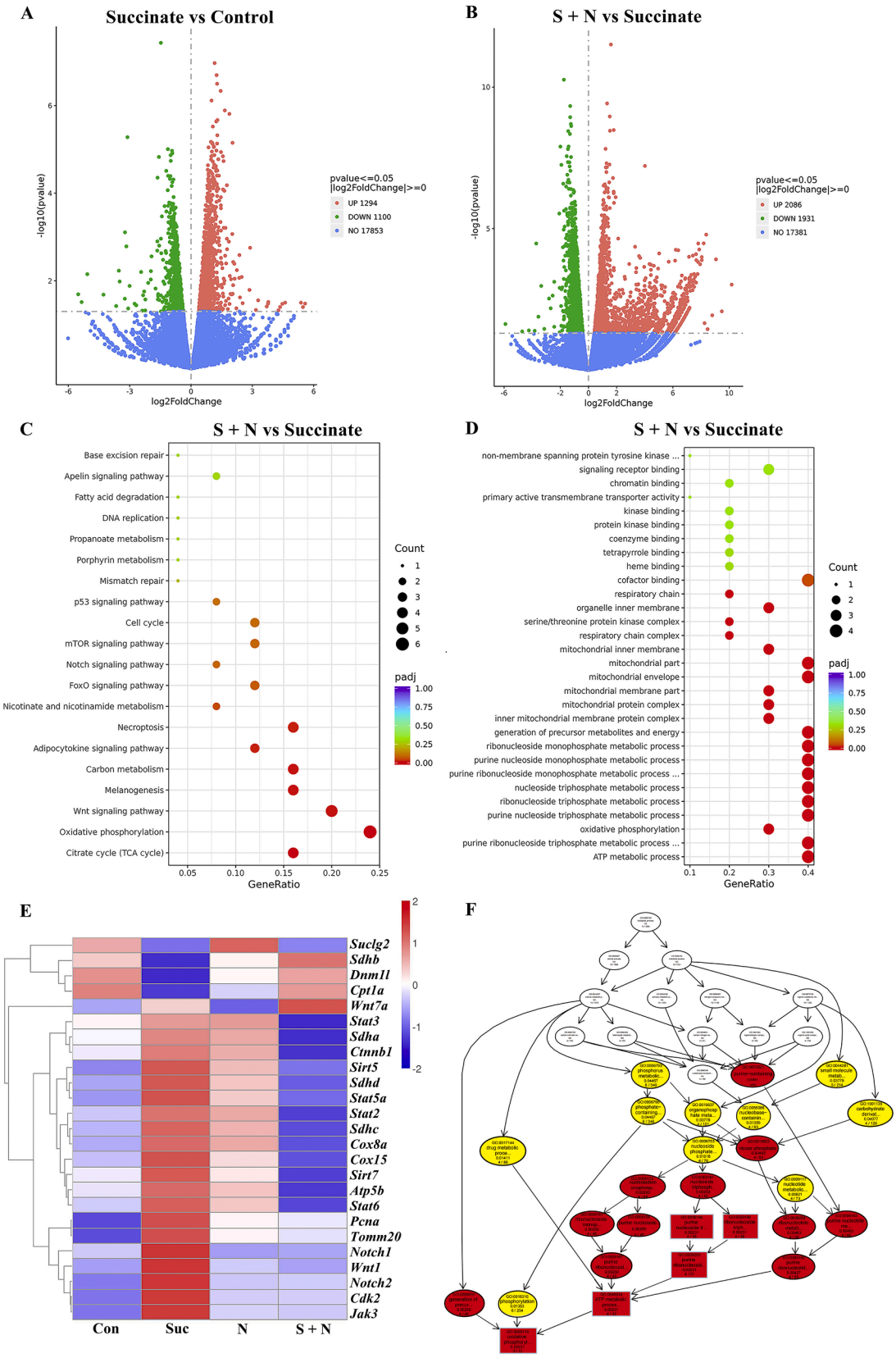

Figure 6. Screening of downstream signaling pathways activated by SUCNR1 in response to succinate. RNA sequencing was performed on enteroids pretreated with an antagonist NF-56-EJ40 followed by succinate treatment. (A-B) The volcano plot displays the differentially expressed genes between the succinate group and the control groups, as well as between the succinate + NF-56-EJ40 group and the succinate group. SN, succinate + NF-56-EJ40. (C-D) KEGG and GO analysis revealed enriched pathways between the succinate + NF-56-EJ40 group and the succinate group. (E) Hierarchical clustering analysis of differentially expressed genes among various groups. (F) Directed Acyclic Graph assay illustrates the functions of the differentially expressed genes. N, NF-56-EJ40. *S* + N, succinate + NF-56-EJ40.

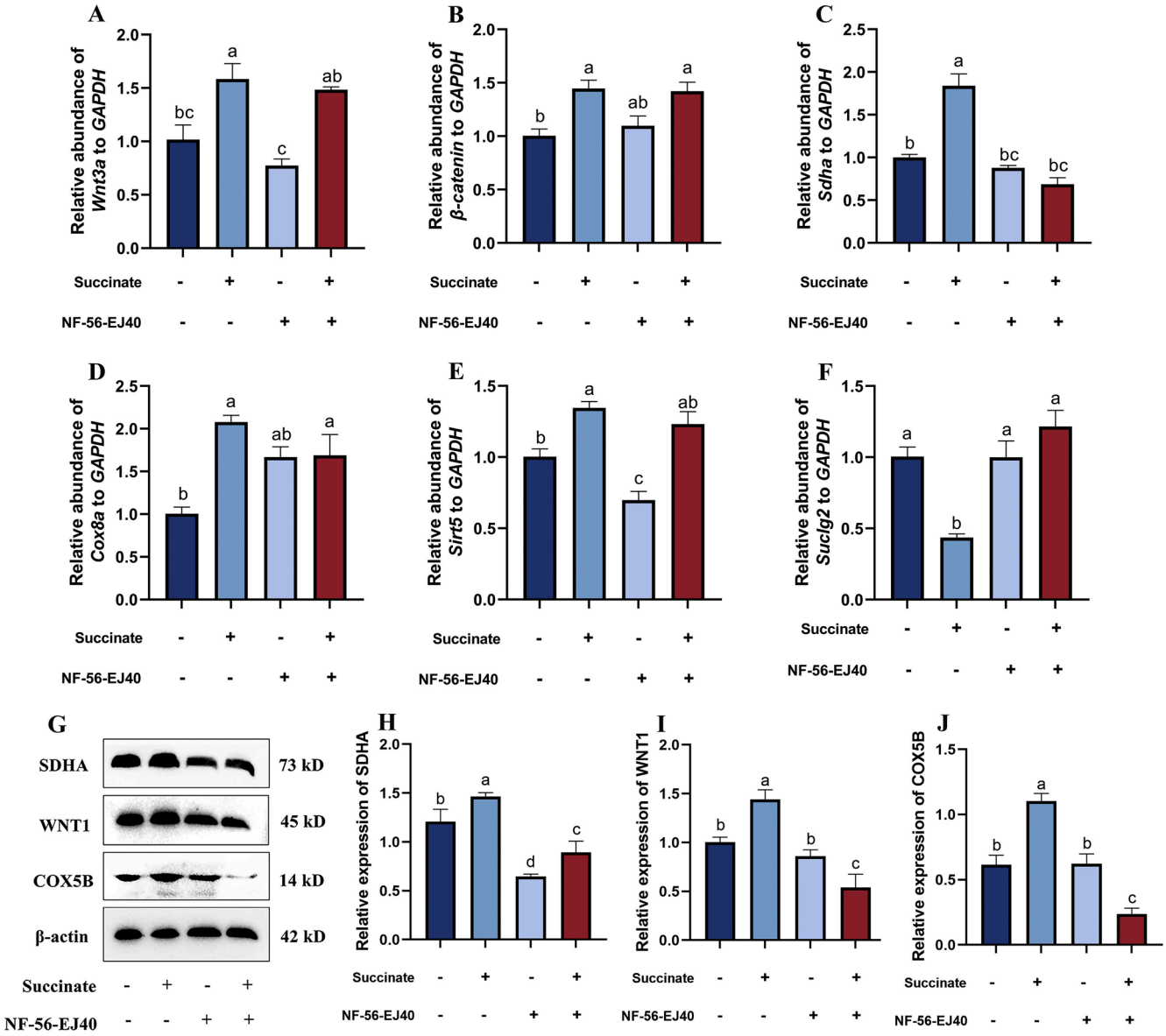

Figure 7. SUCNR1 mediates the effect of succinate on the glycometabolism-related pathway. The enteroids were pretreated with NF-56-EJ40 (SUCNR1 antagonist) followed by succinate treatment. (A-F) Histograms represent mRNA abundance alterations of Wnt3a/β-catenin-related genes (*Wnt3a, β-catenin*), OXPHOS-related enzymes (*Sdha, Cox8a*), desuccinylation-related enzyme (*Sirt5*), and succinylation-related enzyme (*Suclg2*) in enteroids. (G-J) Western blot assay of SDHA, WNT1, and COX5B proteins in enteroids. The data is presented as mean ± standard deviation. Columns without common letters indicate significant differences among the treatments ($P < 0.05$), $n = 3$.

staining assays of LGR5 and TOMM20 in enteroids revealed that pretreatment with the SUCNR1 antagonist NF-56-EJ40 substantially reduced the promotion of mitochondrial fusion by succinate on in ISCs (Fig. 5K). These results confirm that SUCNR1 mediates the effects of succinate on ISC activity and mitochondrial fusion.

Screening of downstream signaling pathways of SUCNR1

To explore the downstream signaling pathway of SUCNR1 that mediates the effects of succinate on ISC activity, RNA sequencing was performed on enteroids. The results from the volcano plot indicate that the succinate group exhibited 1,294 upregulated genes and 1,100 downregulated genes compared to the control group (Fig. 6A), the NF-56-EJ40 + succinate group displayed 2,086 upregulated genes and 1,931 downregulated genes relative to the succinate group (Fig. 6B). Kyoto Encyclopedia of Genes and Genomes (**KEGG**) and Gene Ontology (**GO**) (Fig. 6C and D) revealed that the differentially expressed genes were predominantly enriched in pathways related to oxidative phosphorylation (**OXPHOS**), the tricarboxylic acid (**TCA**) cycle, and the Wnt signaling pathway. Hierarchical clustering analysis of the differentially expressed genes (Fig. 6E) demonstrated that, compared to the control group, succinate notably upregulated numerous genes associated with the Wnt/β-catenin signaling pathways, including Wnt family members 1, 7a (***Wnt1, Wnt7a***) and catenin beta 1 (***β-catenin***). Additionally, genes involved in the TCA cycle and OXPHOS processes, such as succinate dehydrogenase (***Sdh***), cytochrome c oxidase subunits 15, 8a (***Cox15, Cox8a***), and *Atp5b*, were remarkably upregulated. In addition, succinylation-related genes, including splice unified ligand grammar 2 (***Suclg2***) and carnitine palmitoyl-transferase1a (***Cpt1a***), were downregulated, while genes involved in desuccinylation processes, specifically sirtuin5 and sirtuin7 (***Sirt5, Sirt7***), were upregulated. Interestingly, following pre-treatment with the antagonists NF-56-EJ40, the enhancement of succinate on genes associated with Wnt/β-catenin signaling, OXPHOS, TCA cycle, and desuccinylation were completely

abolished. As illustrated in Fig. 6F, the directed acyclic graph (**DAG**) further confirmed that the functions of the differentially expressed genes are dramatically concentrated in OXPHOS.

Succinate activates the glycometabolism-related pathways through SUCNR1

To confirm the glycometabolism-related pathways in enteroids following succinate treatment, we analyzed representative mRNA and protein levels associated with the Wnt/β-catenin pathway, OXPHOS, and succinylation. The results (Fig. 7A-F) indicated that succinate treatment alone increased the mRNA abundance of *Wnt3a* (by 55.65 %, *P*-value = 0.0216) and *β-catenin* (by 43.91 %, *P*-value = 0.0198), increased the mRNA abundance of OXPHOS-related enzymes *Sdha* (by 83.66 %, *P*-value = 0.0004) and *Cox8a* (by 51.58 %, *P*-value = 0.0039), and increased the mRNA abundance of the desuccinylation-related enzyme *Sirt5* by 34.19 % (*P*-value = 0.0230). Conversly, the mRNA abundance of the succinylation-related enzyme *Suclg2* decreased by 56.68 % (*P*-value = 0.0080). Parallelly, as shown in Fig. 7G-J, succinate considerably increased the protein levels of SDHA, WNT1, and COX5B by 21.22 % (*P*-value = 0.0292), 43.67 % (*P*-value = 0.0431) and 79.80 % (*P*-value = 0.0350). Interestingly, upon pre-treating with a SUCNR1 antagonist, compared to succinate treatment alone, the succinate-induced promotion of WNT1 protein level (decreased by 62.59 %, *P*-value = 0.0006), *Sdha* mRNA abundance and SDHA protein level (decreased by 62.69 % and 38.99 %, *P*-value < 0.05), and COX5B protein level (decreased by 78.47 %, *P*-value < 0.0001) disappeared.

Discussion

In the current study, feeding chickens with L. *salivarius* supernatant resulted in a significant upregulation of mRNA abundance for the amino acid transporters *PepT1* and B^0AT. Concurrently, L. *salivarius* supernatant reduced the abundance of intestinal pathogenic bacteria (such as *Desulfovibrio*), while increasing the abundance of probiotics (such as *Verrucomicrobia*). Although 450-day-old laying hens are in the late stage of production, they are still some distance from being culled. Therefore, our study aims to improve the nutrient absorption capacity of late-stage laying hens through the supplementation of succinate, thereby minimizing losses during the production process. In the production of laying hens, egg production sharply declines after reaching a certain point. Our research focuses on delaying the decline in egg production in laying hens rather than increasing the yield of hens that are in their peak production period. Untargeted metabolomic analysis further revealed a high abundance of organic acids, such as malonic acid, folic acid, and succinic acid, in the fermentation supernatant of L. *salivarius*. Moreover, both *in vivo* and *in vitro* studies have further demonstrated that succinate promotes mucosal absorptive capacity, as evidenced by elevated mRNA levels of the amino acid transporters *PepT1*, B^0AT, and *EAAT3*. Previously, it was shown that succinate produced by gut microbiota promotes tuft cell proliferation, thereby alleviating ileitis (Banerjee et al., 2020). Dietary supplementation with succinic acid was adequate to activate a type 2 immune response, induce the differentiation of goblet cells, suppress intestinal inflammation, and restore mucosal barrier impairment induced by a high-fat diet (Li et al., 2023). Succinate has been shown to alleviate intestinal ischemia-reperfusion injury by upregulating krüppel-like factor 4 (***Klf4***), which inhibits necroptosis and inflammation (Cao et al., 2023). The intestinal mucosal absorptive capacity relies on the rapid turnover of the intestinal epithelium. In this study, succinate feeding was confirmed to increase the abundance of cyclin-related *Cdk2* mRNA while decreasing the abundance of apoptosis-related *Bax* mRNA. These findings suggest that succinate may accelerate epithelial turnover, which is well known to depend on the increased activity of ISCs. Our results further confirm that succinate treatment significantly enhances the differentiation and proliferation of ISCs, as evidenced by the elevated protein levels of LGR5 and PCNA. Similarly, our previous study demonstrated that succinate enhance ISC activity in chicken enteroids (Zhou et al., 2022). Therefore, we propose that succinate, a critical metabolite present in the supernatant of L. *salivarius*, can enhance ISC activity and epithelial turnover, thereby improving the absorptive capacity of the intestinal mucosa. Our results indicate that a dosage of 5 mg/kg BW is effective in promoting favorable outcomes for most measured parameters. This suggests that this dosage may serve as a practical and reliable guideline for industrial applications. However, considering the importance of cost-efficiency in large-scale applications, it is worth investigating whether lower dosages, such as less than 5 mg/kg BW, could yield similar benefits. Future studies should focus on exploring the minimum effective dose that balances efficacy and cost-effectiveness, as well as examining the long-term impacts of lower doses on animal health and performance. Such studies would provide valuable insights for refining the practical use of succinate as a feed additive.

Extensive research has demonstrated that the succinate receptor SUCNR1 mediates the effects of extracellular succinate on intracellular signaling cascades. In our study, upon pre-treating with the SUCNR1 antagonist NF-56-EJ40, the enhancement of succinate on ISCs proliferation and differentiation disappeared. Similarly, through SUCNR1, succinate has been shown to promote the migration of hMSCs (Ko et al., 2017), decrease cellular glycolysis in cardiomyocytes (Lu et al., 2018), activate murine tracheal brush cells (Perniss et al., 2023), and enhance intestinal barrier function (Li et al., 2023). Regarding the underlying mechanism by which SUCNR1 mediates alterations in ISC activity, growing evidence indicated that mitochondria determine cell fate through dynamic transformations involving fusion and fission. Our study further confirmed that in enteroids, succinate increases the protein levels of OPA1 and TOMM20, which promote mitochondrial fusion, as well as elevated ATP content. This suggests that succinate could promote mitochondrial fusion and energy metabolism in enteroids. However, pre-treatment with NF-56-EJ40 significantly reduced the effects of succinate on mitochondrial fusion and local ATP levels. Furthermore, a co-staining assay of LGR5 and TOMM20 in enteroids confirmed that pre-treatment with a SUCNR1 antagonist reduced the effects of succinate on mitochondrial fusion in ISCs. Consistent with this, an the imbalance between mitochondrial fusion and fission can impair the intestinal epithelial barrier function in pigs (Zhang et al., 2022). In mice, mitochondria within ISCs exhibit high activity and generate mitochondrial reactive oxygen species (mtROS) through OXPHOS, which is crucial for driving the self-renewal and differentiation of $Lgr5^+$ ISCs (Rodríguez-Colman et al., 2017). A decline in OPA1 expression and disrupted mitochondrial dynamics can lead to age-related dysfunction of muscle stem cells (MuSCs) (Baker et al., 2022). OPA1, a key regulator of mitochondrial dynamics, promotes ferroptosis by maintaining mitochondrial function and homeostasis (Liang et al., 2024). Leptin enhances glycolysis through OPA1-mediated mitochondrial fusion, promoting the survival of mesenchymal stem cells (Yang et al., 2019). Taken together, our results suggest that SUCNR1 mediates the effects of succinate in promoting mitochondrial fusion in ISCs, thereby further regulating ISC activity.

In the case of the signaling pathway through which SUCNR1 regulates mitochondrial fusion, our study identified that genes associated with Wnt/β-catenin signaling were activated. To identifying the optimal dosage at which NF-56-EJ40 inhibits the effects of succinate, enteroids were pre-treated with NF-56-EJ40 at concentrations of 2.5 μM, 5 μM, or 10 μM for 30 min. In this study, genes linked to Wnt/β-catenin signaling were identified using RNA sequencing, qPCR, and Western blot assays. Additionally, succinate and SUCNR1 were found to be upregulated in the vicinity of Crohn's disease (CD) fistulas, further activating Wnt signaling and inducing epithelial-to-mesenchymal transition in the intestinal epithelium (Ortiz-Masiá et al., 2020). Transmissible gastroenteritis virus (TGEV) infection activates the Wnt/β-catenin pathway, promoting ISC self-renewal and leading to intestinal epithelial regeneration (Yang et al., 2022). Importantly, our screening further confirmed

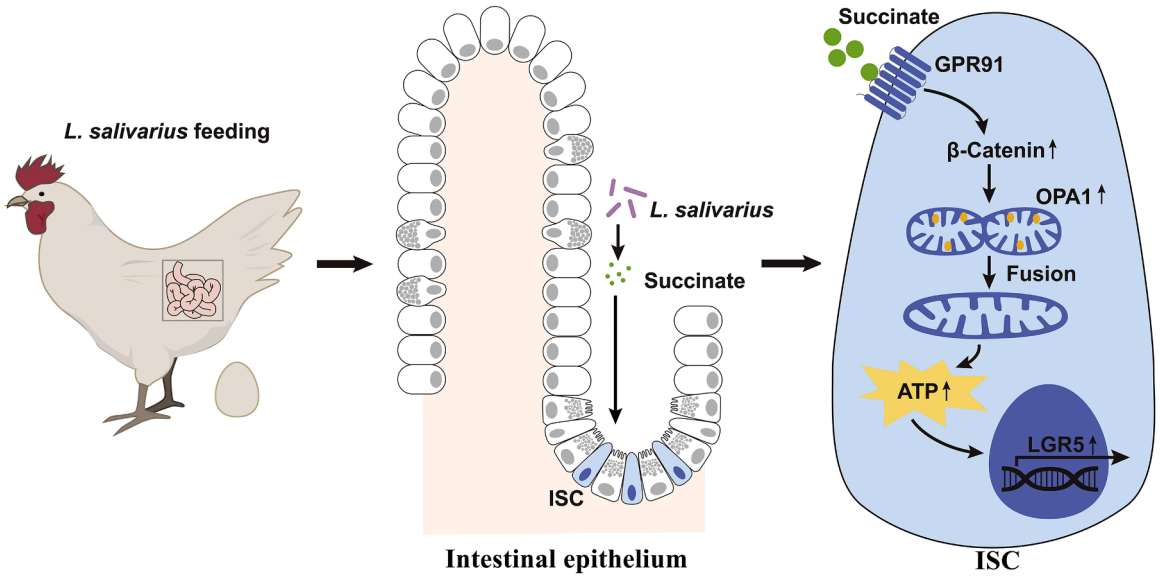

Figure 8. Schematic representations of the main findings in this work. Succinate, a metabolite of L. *salivarius*, plays a crucial role in activating the SUCNR1-mitochondria axis in ISC, which further promotes mitochondrial fusion, ATP synthesis, and enhances ISC differentiation and proliferation. Ultimately, this process leads to accelerated turnover of the epithelium, enhancing mucosal absorptive capacity.

that succinate activates the glycometabolism-related pathways, particularly those involving *Sdh, Cox15, Cox8a*, and *Atp5b*, which are associated with OXPHOS. Meanwhile, NF-56-EJ40 diminishes the enhancement of succinate on succinylation-related genes (*Suclg2* and *Cpt1a*), suggesting that succinate inhibits succinylation in ISCs. Furthermore, the beneficial gut fungus *Kazachstania slooffiae* has been shown to enhance porcine intestinal epithelial glycolysis through lysine desuccinylation (Hu et al., 2023a). SUCLG2 plays a critical role in regulating mitochondrial dysfunction and succinylation in lung adenocarcinoma, highlighting its involvement in protein stability and metabolic reprogramming during cancer progression (Hu et al., 2023b). Therefore, we propose that the Wnt/β-catenin pathway serves as a downstream signal of SUCNR1, which can be activated by succinate, further inducing mitochondrial fusion, inhibiting succinylation, enhancing OXPHOS levels, and increasing ATP content, ultimately boosting ISC activity.

In summary, our study confirms that the fermentation supernatant of L. *salivarius* enhances the absorptive capacity of the intestinal mucosal. Among the metabolites present in L. *salivarius* supernatant, succinate plays a crucial role in activating the SUCNR1-mitochondria axis and promoteing mitochondrial fusion, OXPHOS levels, and ATP synthesis in the crypt (Fig. 8). Thus, promoting ISC activity, and ultimately enhancing mucosal absorptive capacity.

Availability of data and material

The authors confirm that the data supporting the findings of this study are available within the article. The datasets supporting the conclusions of this article are available in the NCBI BioProject no. PRJNA1117850, PRJNA735554 and PRJNA1118057.

Ethics approval

This study was conducted following the *Guiding Principles for the Care and Use of Laboratory Animals* as adopted by Zhejiang University. Approval for the experimental procedures was granted by *Zhejiang University's Committee on the Ethics of Animal Experiments* (Approval No. 14933).

Declaration of competing interest

The authors report there are no competing interests to declare.

Acknowledgments

D. Luo conducted the experiments, collected and analyzed the data, and wrote the manuscript. M. Zou, L. Zhang, Y. Hua, and L. Yu were responsible for part of enteroids culture and molecular biology experiments. X. Rao, M. Wei, J. Cao, J. Ye and S. Qi were responsible for the animal experiments. H. Wang, Y. Mi and C. Zhang were responsible for data interpretation and manuscript revision. J. Li was responsible for the conception and design of the study, analysis and interpretation of data, and final approval of the version submitted. All authors reviewed the manuscript. We are grateful to Weidong Zeng (Zhejiang University) and the Experimental Teaching Center (College of Animal Sciences, Zhejiang University) for help in the experiments.

FUNDING

This study was supported by the program of the Zhejiang Provincial Department of Agriculture and Rural Affairs (2024SNJF046), the National Natural Science Foundation of China (No. 31972630), the Basic Public Welfare Research Program of Zhejiang Provincial (No. LGN21C180003), and the Scientific Research Fund of Zhejiang University (No. XY2023006).

References

Baker, N., Wade, S., Triolo, M., Girgis, J., Chwastek, D., Larrigan, S., Feige, P., Fujita, R., Crist, C., Rudnicki, M.A., Burelle, Y., Khacho, M., 2022. The mitochondrial protein OPA1 regulates the quiescent state of adult muscle stem cells. Cell Stem. Cell 29, 1315–1332 e9.

Banerjee, A., Herring, C.A., Chen, B., Kim, H., Simmons, A.J., Southard-Smith, A.N., Allaman, M.M., White, J.R., Macedonia, M.C., Mckinley, E.T., Ramirez-Solano, M.A., Scoville, E.A., Liu, Q., Wilson, K.T., Coffey, R.J., Washington, M.K., Goettel, J.A., Lau, K.S., 2020. Succinate produced by intestinal microbes promotes specification of tuft cells to suppress ileal inflammation. Gastroenterology 159, 2101–2115 e5.

Cao, Z., Mu, S., Wang, M., Zhang, Y., Zou, G., Yuan, X., Huang, Y., Yu, S., Zhang, J., Zhang, C., 2023. Succinate pretreatment attenuates intestinal ischemia-reperfusion injury by inhibiting necroptosis and inflammation via upregulating Klf4. Int. Immunopharmacol 120, 110425.

Che, Y., Xu, W., Ding, C., He, T., Xu, X., Shuai, Y., Huang, H., Wu, J., Wang, Y., Wang, C., Wang, G., Cao, L., Hao, H., 2023. Bile acids target mitofusin 2 to differentially

regulate innate immunity in physiological versus cholestatic conditions. Cell Rep 42, 112011.
Chen, L., Li, S., Peng, C., Gui, Q., Li, J., Xu, Z., Yang, Y., 2023. *Lactobacillus rhamnosus* GG promotes recovery of the colon barrier in septic mice through accelerating iscs regeneration. Nutrients 15, 672.
Connors, J., Dawe, N., Van Limbergen, J., 2018. The role of succinate in the regulation of intestinal inflammation. Nutrients 11, 25.
Deng, H., Takashima, S., Paul, M., Guo, M., Hartenstein, V., 2018. Mitochondrial dynamics regulates *Drosophila* intestinal stem cell differentiation. Cell Death Discov 4, 17.
Dubal, D., Moghe, P., Verma, R.K., Uttekar, B., Rikhy, R., 2022. Mitochondrial fusion regulates proliferation and differentiation in the type II neuroblast lineage in *Drosophila*. PLoS. Genet 18, e1010055.
Hu, J., Chen, J., Hou, Q., Xu, X., Ren, J., Ma, L., Yan, X., 2023a. Core-predominant gut fungus kazachstania slooffiae promotes intestinal epithelial glycolysis via lysine desuccinylation in pigs. Microbiome 11, 31.
Hu, Q., Xu, J., Wang, L., Yuan, Y., Luo, R., Gan, M., Wang, K., Zhao, T., Wang, Y., Han, T., Wang, J.-B., 2023b. SUCLG2 regulates mitochondrial dysfunction through succinylation in lung adenocarcinoma. Adv. Sci. (Weinh) 10, e2303535.
Khan, R.U., Naz, S.., Raziq, F., Qudratullah, Q., Khan, N.A., Laudadio, V., Tufarelli, V., Ragni, M., 2022. Prospects of organic acids as safe alternative to antibiotics in broiler chickens diet. Environ. Sci. Pollut. Res 29, 32594–32604.
Ko, S.H., Choi, G..E., Oh, J.Y., Lee, H.J., Kim, J.S., Chae, C.W., Choi, D., Han, H.J., 2017. Succinate promotes stem cell migration through the GPR91-dependent regulation of DRP1-mediated mitochondrial fission. Sci. Rep 7, 12582.
Li, X., Huang, G., Zhang, Y., Ren, Y., Zhang, R., Zhu, W., Yu, K., 2023. Succinate signaling attenuates high-fat diet-induced metabolic disturbance and intestinal barrier dysfunction. Pharmacol. Res 194, 106865.
Li, J., Li, J., Zhang, S.Y., Li, R.X., Lin, X., Mi, Y.L., Zhang, C.Q., 2018. Culture and characterization of chicken small intestinal crypts. Poult. Sci 97, 1536–1543.
Li, X., Mao, M., Zhang, Y., Yu, K., Zhu, W., 2019. Succinate modulates intestinal barrier function and inflammation response in pigs. Biomolecules 9, 486.
Liang, F.G., Zandkarimi, F., Lee, J., Axelrod, J.L., Pekson, R., Yoon, Y., Stockwell, B.R., Kitsis, R.N., 2024. OPA1 promotes ferroptosis by augmenting mitochondrial ROS and suppressing an integrated stress response. Mol. Cell 84, 3098–3114 e6.
Liu, L., Zhou, Z., Hong, Y., Jiang, K., Yu, L., Xie, X., Mi, Y., Zhu, S.J., Zhang, C., Li, J., 2022. Transplantion of predominant *lactobacilli* from native hens to commercial hens could indirectly regulate their ISC activity by improving intestinal microbiota. Microb. Biotechnol 15, 1235–1252.
Lu, Y.-T., Li, L.-Z., Yang, Y.-L., Yin, X., Liu, Q., Zhang, L., Liu, K., Liu, B., Li, J., Qi, L.-W., 2018. Succinate induces aberrant mitochondrial fission in cardiomyocytes through GPR91 signaling. Cell Death Dis 9, 672.
Mancini, N.L., Rajeev, S.., Jayme, T.S., Wang, A., Keita, Å.V., Workentine, M.L., Hamed, S., Söderholm, J.D., Lopes, F., Shutt, T.E., Shearer, J., McKay, D.M., 2021. Crohn's disease pathobiont adherent-invasive *E coli* disrupts epithelial mitochondrial networks with implications for gut permeability. Cell Mol. Gastroenterol. Hepatol 11, 551–571.
Noone, J., O'Gorman, D.J., Kenny, H.C., 2022. OPA1 regulation of mitochondrial dynamics in skeletal and cardiac muscle. Trends Endocrinol. Metab 33, 710–721.
Ortiz-Masiá, D., Gisbert-Ferrándiz, L., Bauset, C., Coll, S., Mamie, C., Scharl, M., Esplugues, J.V., Alós, R., Navarro, F., Cosín-Roger, J., Barrachina, M.D., Calatayud, S., 2020. Succinate activates emt in intestinal epithelial cells through SUCNR1: a novel protagonist in fistula development. Cells 9, 1104.
Perniss, A., Boonen, B., Tonack, S., Thiel, M., Poharkar, K., Alnouri, M.W., Keshavarz, M., Papadakis, T., Wiegand, S., Pfeil, U., Richter, K., Althaus, M., Oberwinkler, J., Schütz, B., Boehm, U., Offermanns, S., Leinders-Zufall, T., Zufall, F., Kummer, W., 2023. A succinate/SUCNR1-brush cell defense program in the tracheal epithelium. Sci. Adv 9, eadg8842.
Rodríguez-Colman, M.J., Schewe, M.., Meerlo, M., Stigter, E., Gerrits, J., Pras-Raves, M., Sacchetti, A., Hornsveld, M., Oost, K.C., Snippert, H.J., Verhoeven-Duif, N., Fodde, R., Burgering, B.M.T., 2017. Interplay between metabolic identities in the intestinal crypt supports stem cell function. Nature 543, 424–427.
Villanueva-Carmona, T., Cedó, L., Madeira, A., Ceperuelo-Mallafré, V., Rodríguez-Peña, M.-M., Núñez-Roa, C., Maymó-Masip, E., Repollés-de-Dalmau, M., Badia, J., Keiran, N., Mirasierra, M., Pimenta-Lopes, C., Sabadell-Basallote, J., Bosch, R., Caubet, L., Escolà-Gil, J.C., Fernández-Real, J.-M., Vilarrasa, N., Ventura, F., Vallejo, M., Vendrell, J., Fernández-Veledo, S., 2023. SUCNR1 signaling in adipocytes controls energy metabolism by modulating circadian clock and leptin expression. Cell Metab 35, 601–619 e10.
Wang, D., Kuang, Y., Wan, Z., Li, P., Zhao, J., Zhu, H., Liu, Y., 2022. Aspartate alleviates colonic epithelial damage by regulating intestinal stem cell proliferation and differentiation via mitochondrial dynamics. Mol. Nutr. Food Res 66, e2200168.
Wu, H., Xie, S., Miao, J., Li, Y., Wang, Z., Wang, M., Yu, Q., 2020. *Lactobacillus reuteri* maintains intestinal epithelial regeneration and repairs damaged intestinal mucosa. Gut. Microbes 11, 997–1014.
Yan, X.-L., Liu, X.-C., Zhang, Y.-N., Du, T.-T., Ai, Q., Gao, X., Yang, J.-L., Bao, L., Li, L.-Q., 2022. Succinate aggravates intestinal injury in mice with necrotizing enterocolitis. Front. Cell Infect. Microbiol 12, 1064462.
Yang, F., Li, B., Yang, Y., Huang, M., Liu, X., Zhang, Y., Liu, H., Zhang, L., Pan, Y., Tian, S., Wu, Y., Wang, L., Yang, L., 2019. Leptin enhances glycolysis via OPA1-mediated mitochondrial fusion to promote mesenchymal stem cell survival. Int. J. Mol. Med 44, 301–312.
Yang, N., Zhang, Y., Fu, Y., Li, Y., Yang, S., Chen, J., Liu, G., 2022. Transmissible gastroenteritis virus infection promotes the self-renewal of porcine intestinal stem cells via wnt/β-catenin pathway. J. Virol 96, e0096222.
Zhang, C., Zhang, K.-F., Chen, F.-J., Chen, Y.-H., Yang, X., Cai, Z.-H., Jiang, Y.-B., Wang, X.-B., Zhang, G.-P., Wang, F.-Y., 2022. Deoxynivalenol triggers porcine intestinal tight junction disorder: iinsights from mitochondrial dynamics and mitophagy. Ecotoxicol. Environ. Saf 248, 114291.
Zhou, Z., Yu, L., Cao, J., Yu, J., Lin, Z., Hong, Y., Jiang, S., Chen, C., Mi, Y., Zhang, C., Li, J., 2022. Lactobacillus salivarius promotion of intestinal stem cell activity in hens is associated with succinate-induced mitochondrial energy metabolism. mSystems 7, e00903–e00922.